Microelectronics Reliability 114 (2020) 113799

Contents lists available at ScienceDirect

Microelectronics Reliability

journal homepage: www.elsevier.com/locate/microrel

Prediction of solar particle events with SRAM-based soft error rate monitor and supervised machine learning

J. Chen[a,*], T. Lange[b,d], M. Andjelkovic[a], A. Simevski[a], M. Krstic[a,c]

[a] IHP – Leibniz-Institut für innovative Mikroelektronik, Frankfurt Oder, Germany
[b] iROC, Grenoble, France
[c] University of Potsdam, Potsdam, Germany
[d] Politecnico de Torino, Torino, Italy

A B S T R A C T

This work introduces an embedded approach for the prediction of Solar Particle Events (SPEs) in space applications by combining the real-time Soft Error Rate (SER) measurement with SRAM-based detector and the offline trained machine learning model. The proposed approach is intended for the self-adaptive fault-tolerant multiprocessing systems employed in space applications. With respect to the state-of-the-art, our solution allows for predicting the SER 1 h in advance and fine-grained hourly tracking of SER variations during SPEs as well as under normal conditions. Therefore, the target system can activate the appropriate mechanisms for radiation hardening before the onset of high radiation levels. Based on the comparison of five different machine learning algorithms trained with the public space flux database, the preliminary results indicate that the best prediction accuracy is achieved with the recurrent neural network (RNN) with long short-term memory (LSTM).

1. Introduction

The Solar Particle Events (SPEs) represent the periods of intense radiation bursts resulting from solar storms on the Sun's surface [1]. During these events, the energetic particles such as heavy ions and protons are emitted in space, and the particle fluxes are orders of magnitude higher than the background level. These particles pose a severe reliability threat for electronics employed in space missions. Namely, the passage of an energetic particle through the sensitive region of a digital circuit may cause the Single Event Upsets (SEUs), i.e. temporary bit flips in storage elements (flip-flops, latches and SRAM cells). The SEUs (also known as soft errors) may result in malfunction and failure of the complete system. It is therefore essential to provide efficient mitigation of SEUs in electronic systems intended for space applications.

According to data from various space missions [2,3], the SEU rate for commercial Static Random Access Memories (SRAMs) can increase by several orders of magnitude during the SPEs. Since the high radiation levels during an SPE can last for hours or even days [4], it is vital to detect the changes in the radiation exposure and activate the suitable radiation hardening measures to protect the critical elements of the system. A typical solution would be in the use of adaptive multi-core processing system based on configuring the cores into a rad-hard mode (e.g. Triple Modular Redundancy) when the high radiation levels are detected. Alternatively, under low radiation levels the cores can be configured for high performance or low power consumption, as required by the application [5]. This concept enables to achieve the optimum system performance with highest possible robustness to ionizing radiation and minimum power consumption under variable operating conditions.

The detection of SPEs is achieved with particle detectors which allow for measuring the soft error rate (SER) in terms of the particle flux in real-time. Once the particle flux and SER are determined under given radiation conditions, the suitable hardening measure can be activated. However, in order to achieve efficient SEU mitigation and prevent the data loss, it is important to be able to predict the increase in particle flux or SER, i.e. to predict when an SPE will occur. To accomplish this, various machine learning algorithms can be applied to train the system for predicting the variations of SER from the real-time SER measurements.

Numerous works have reported the use of different machine learning algorithms to predict the onset and duration of SPEs for various purposes such as space weather forecasting, planning the spacecraft and satellite routes/manoeuvers, protection of astronauts in space missions, etc. [6–9]. The machine learning algorithms have been also used for optimization of the SER characterization in the rad-hard system design phase [10–12]. Furthermore, the use of machine learning for dynamic control of the fault tolerant mechanisms in cyber security

* Corresponding author.
E-mail addresses: chen@ihp-microelectronics.com (J. Chen), lange@ihp-microelectronics.com (T. Lange), andjelkovic@ihp-microelectronics.com (M. Andjelkovic), simevski@ihp-microelectronics.com (A. Simevski), krstic@ihp-microelectronics.com (M. Krstic).

https://doi.org/10.1016/j.microrel.2020.113799
Received 29 May 2020; Received in revised form 9 July 2020; Accepted 14 July 2020
Available online 31 October 2020

applications has been reported [13].

However, to the best of our knowledge, there is no much of publicly available work on the use of machine learning algorithms for predicting the SPEs from in-flight SER data, as a means of enabling the self-adaptive fault tolerance in space systems. This issue has been addressed to a certain extent in [4], where the BRAMs embedded in an FPGA are used as particle detectors and the SPE onset is detected by measuring four SER values to calculate the mean time between failures. Such concept allows only to classify the SPE into five static levels but the real-time variations of the SPE cannot be monitored. Moreover, due to the variable detection time which depends on the mean time between failures, some SPE peak values may not be detected [4].

In contrast to the approach in [4], this work proposes the use of an embedded on-chip SRAM as a particle detector and the supervised machine learning model to predict the SER of SRAM and thus the occurrence of an SPE. Our solution enables to predict the hourly changes of SER, providing a fine-grained representation of the SER variation at least 1 h in advance. Moreover, the prediction period does not depend on the measured real-time SER, which eliminates the risk of not detecting the presence of SPE. The importance of such solution is the fact that the ability to predict the increased radiation levels minimizes the risk that the target system will be exposed to adverse conditions without being sufficiently protected.

The rest of the paper is structured as follows. Section 2 gives a brief description of the proposed method. Section 3 explains the analysis procedure of historical solar condition, i.e. how the SEU rate is extracted from the available database. The machine learning models and training results are detailed in Section 4. The conclusion and main direction for future work are outlined in Section 5.

2. Proposed approach

In Fig. 1, our approach for the prediction of SPEs is illustrated. The main idea is based on the prediction of SER of an on-board SEU monitor, and the rise of SER is used as the indication for an upcoming SPE. Thus, the two main phases in the proposed SPE prediction approach are:

- *Online phase* – measurement of SER (SEU rate) of an SRAM-based SEU monitor in real-time and prediction of SER variations.
- *Offline phase* – use of historical hourly flux data to establish/train a SER prediction model.

The online SER measurement is conducted continuously during the mission. Important is to mention that the existing functional SRAM resource are used for the real-time SER measurement. A detailed description of the corresponding concept can be found in our work [14]. Based on the prediction model and the real-time measurements of SER, the expected SER of the SEU monitor in the following hour can be predicted. Since the SER of an electronic system exposed to radiation is linearly related to the particle flux [15], the predicted SER information should then be used to estimate the SER of the target fault tolerance system, but this is beyond the scope of this work. The hardware design for the prediction block, which implements the trained machine learning model from the offline phase, is also not the scope of current work.

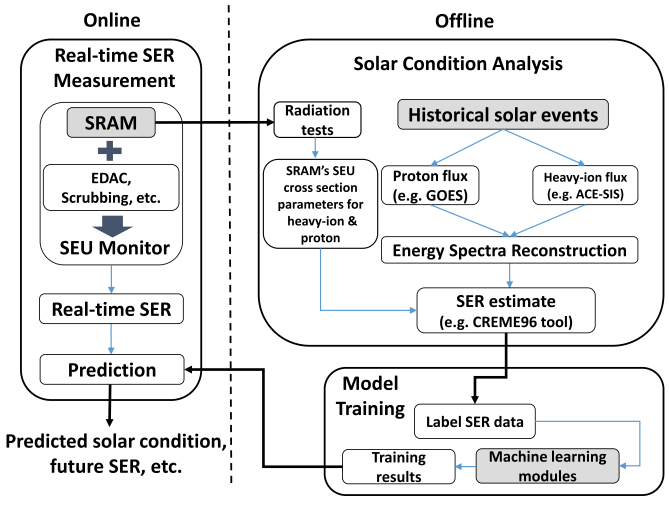

Fig. 1. Proposed SPE prediction flow.

The offline phase performs two main tasks: *historical solar condition analysis* and *prediction model training*. In the historical solar condition analysis, several SPEs are analysed and the corresponding hourly SER data of selected SRAM is collected, which is discussed in Section 3. The hourly SER data is used to train and validate the machine learning models, as described in Section 4.

3. Solar condition analysis

In this section, the procedure to obtain the in-flight SER data using real historical SPE flux data is described. The general steps of the procedure are:

(1) Collection of historical solar events flux data;
(2) SPE energy spectra reconstruction;
(3) SER estimation.

3.1. Flux data collection

The data on the past solar activities, collected by the orbital satellites, is publicly available and can serve as a basis for the offline analysis of solar activities and prediction of SPEs for future missions. According to the large events list from the National Oceanic and Atmospheric Administration (NOAA) [16], all 36 SPEs which occurred during the solar cycle 24 (2008–2019) are selected for this analysis. The Geostationary Operational Environmental Satellite-Space Environment Moni-tor (GOES-SEM) database [17], which continuously provides the data since 1974, has been selected as the proton data source. The Advanced Composition Explorer-Solar Isotope Spectrometer (ACE-SIS) database, which continuously provides the [He, C, N, O, Ne, Na, Ma, Al, Si, S, Ar, Ca, Fe and Ni] flux data since 1997, has been chosen for heavy-ion data source [18]. The working environments for the GOES and ACE satellites are close to the Earth in the heliosphere, but outside the Earth's geomagnetic influence. Therefore, the additional radiation impact from geomagnetically trapped protons and the shield protection from the Earth's magnetic field can be neglected during the following SER calculation.

3.2. SPE energy spectra reconstruction

The flux data obtained from online databases cannot be used directly for the SER estimation due to the data gaps, low energy range and incomplete ion type measurements. Therefore, the common approach to address the above issues is to generate the missing ion fluxes from composition ratios with existing flux information [19].

In this study, due to the incomplete ion types, the heavy-ion induced SEU rate calculation by using only the ACE-SIS ions has the error of about 6%. Moreover, the energy range from ACE-SIS is from 5 to 150 MeV, which is insufficient for SEU rate estimations. Therefore, the energy spectrum has to be extrapolated to a higher range, i.e. from 1 to 10 GeV. The first order power-law fit is used for heavy-ion energy spectra in this study, which can provide a good fluencies in the high-energy range. Different from the data from ACE-SIS, the proton data from GOES database has a good quality and energy range, which is over 700 MeV. To ensure the estimation of proton energy spectra in the same range as heavy-ion, the exponential in particle rigidity fitting method

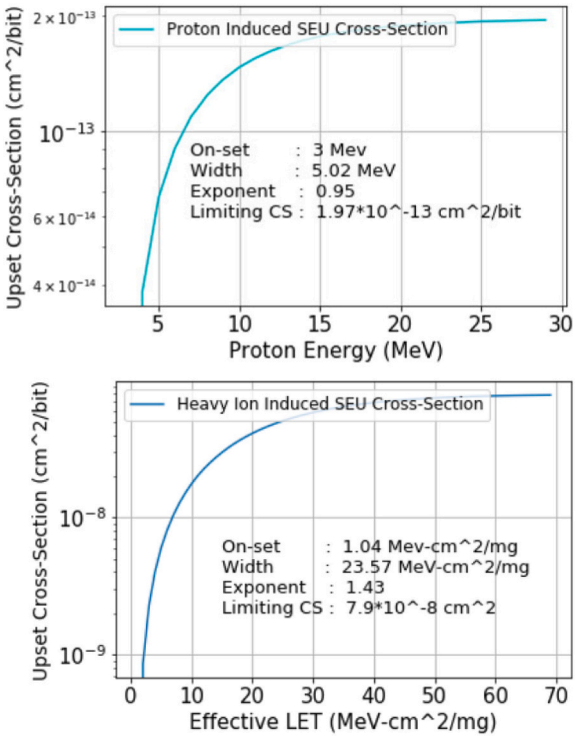

Fig. 2. Weibull fit curves and parameters for the proton and heavy-ion experimental SEU cross-section measurements of the 65 nm SRAM from Cypress.

and the first-order power-law method are used for lower and higher (HEPAD energy channels, larger than 375 MeV for GOES 15) energy range fitting, respectively. The detailed description of the above energy spectra reconstruction methods can be found in [19].

3.3. SER estimation

The CREME96 [20,21] suit was used for estimation of hourly SER of SRAM-based SEU monitor. It is an update of the Cosmic Ray Effects on Micro-Electronics code, and is one of the most widely used suites for creating the ionizing radiation environment models and evaluating the in-orbit soft error rate for space applications.

The SRAM used in this study is a 65 nm COTS SRAM in bulk technology from Cypress. Fig. 2 shows the Weibull fit for heavy-ion and proton cross-section curves for the target SRAM obtained from radiation tests [22].

In the CREME96, the environmental models are generated from each selected event ion fluxes and with 100 mils of device shielding before the SER calculation, which is a conventional equivalent shielding thickness for spacecraft [22]. Since the heavy-ion induced upsets depend on the energy deposition, but not the number of hits like proton-induced upsets, the Sensitive Volume (SV) geometry is necessary for the following calculation [23]. The CREME96 uses the RPP model (Rectangular Parallelepiped Parallelogram) [24] for direct ionization induced upset events calculation, in which the bit SV is assumed to have this shape. Choosing the RPP thickness that conforms to the device cross-section direction dependence is not trivial [25].

For simplicity, we choose the recommended RPP value in CREME96, in which lateral dimensions x and y are determined as the square root of the limiting cross-section for each bit, and the device depth z is 0.5 um. The limiting (saturation) cross-section is obtained from the Weibull fitting as shown in Fig. 2. Using the above values, the in-flight SER data of the target SRAM during the selected SPEs can be calculated from CREME96. Figs. 3 and 4 present the obtained proton-induced and heavy-ion-induced hourly SER respect to the corresponding ion flux from March 6 to 10, 2012, respectively. The observed SER for the target SRAM on the monitor is the sum of the calculated proton and heavy-ion induced SER.

4. SER prediction with machine learning

The aim of the presented approach is to obtain a model which is able to predict fine-grained SER 1 h in advance. For this purpose, the use of machine learning models is investigated in this section. Since the prediction is intended to operate in conjunction with the real-time SER measurement, regression models are used to predict the future SER values.

The analysed machine learning models were chosen based on the low-resources requirement. The models are trained in a supervised manner and the training can be conducted off-line by using the in-flight data from historical solar events (as described in section 3.). This allows to use a trained model for the on-line prediction which usually requires fewer computation resources. In the following, the model training and evaluation methodology are described and the model performances to predict future SER values are evaluated. Therefore, the hourly SER data set (obtained as described in Section 3.) is split into training (60%) and test data set (40%). The training data is used to train the machine learning models and the test data set to measure the performance of the prediction.

4.1. Model training and hyperparameter optimization

Usually, machine learning models are represented by internal parameters or an internal state. These internal parameters or this state are determined during the training process by the machine learning algorithm. Additionally, most of the machine learning algorithms can be controlled by hyperparameters. In contrast to the internal parameters or the state, these hyperparameters are not derived by the training algorithm and need to be set manually before the training process. The problem of finding the optimal set of hyperparameters for the model is called hyperparameter optimization. Therefore, several instances of the model need to be trained and evaluated for different tuples of hyperparameters. The tuple that minimizes a predefined loss function or evaluation metrics yields an optimal model. A random search method combined with a grid search method is a common approach to perform the optimization. There, the model is first evaluated for parameter values randomly generated in a given distribution. Afterwards, a more detailed grid search is performed within the region of the values obtained by the random search [26].

Additionally, to the hyperparameters, the optimal length for the historical hourly SER data needs to be determined. Therefore, models were also evaluated for different history length of the hourly SER data.

4.2. Model evaluation

To measure the performance of the selected models the models are predicting the SER values of the test data set. This prediction is compared against actual values and quantified by using different metrics: The mean absolute error (MAE), the maximum absolute error (MAX), the root-mean-square error (RMSE), and the coefficient of determination (R2) are used.

This ensures that the model is not only trained for one particular training and test data set, but the performance is also measured by using cross-validation. In this approach, the model is trained and evaluated against multiple train and test splits of the data. Several subsets, or cross-validation folds, of the data set, are created and each fold is used to train and evaluate a separate model. Then the average across the folds is calculated and thus, instead of relying only on one single training and test data set, a more stable performance measure is obtained which indicates how the model is likely to perform on average [27].

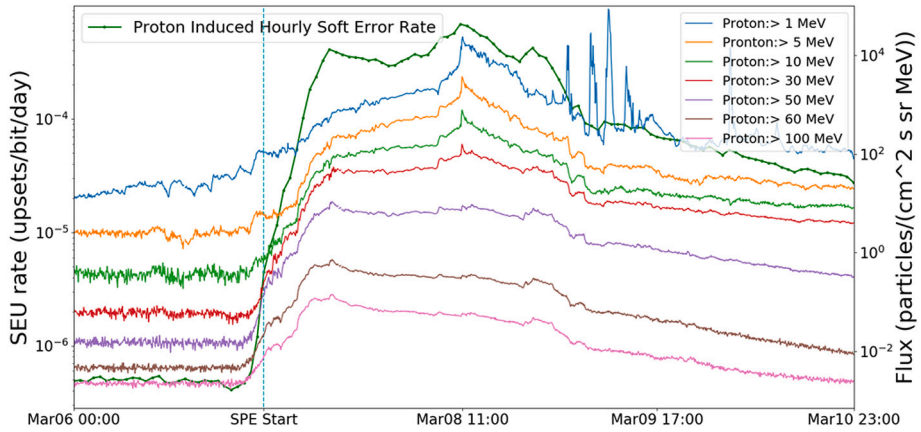

Fig. 3. Proton-induced SER (SEU rate) from GOES database for March 6–10, 2012. The particle flux for all of the lower to higher energy channels are shown, and all channels are with good quality.

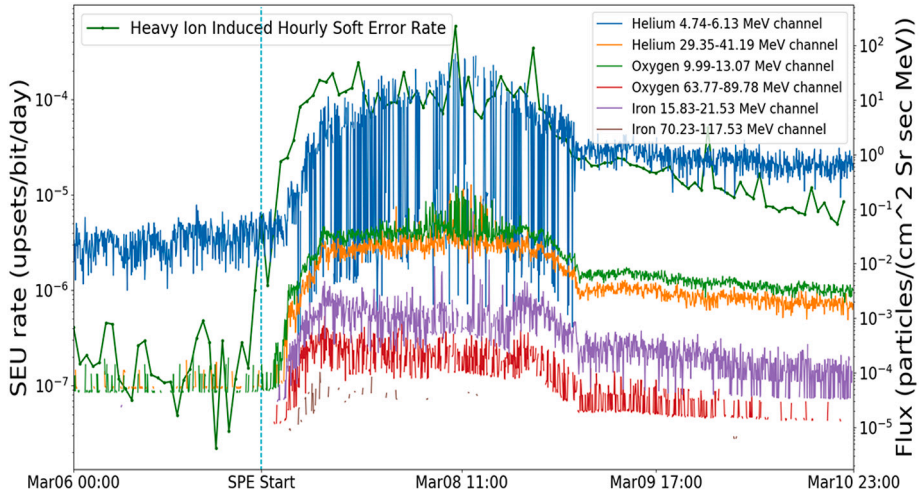

Fig. 4. Heavy-ion-induced SER (SEU rate) from ACE-SIS database for March 6–10, 2012. The particle ion flux of He, O and Fe for the lower and higher energy channels are shown, and high-energy channels data are of poor quality.

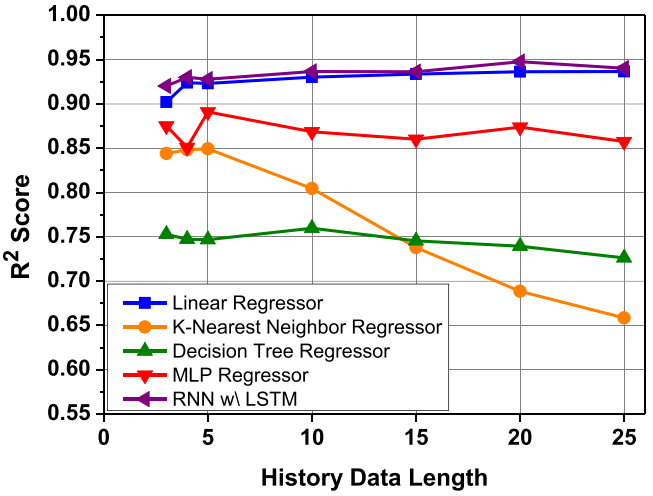

Fig. 5. R^2 score for selected models in terms of history data length.

4.3. Evaluated regression models

For the analysis in this paper the following five regression models have been considered: (1) linear least squares regression, (2) decision tree regression, (3) k-nearest neighbors regression, (4) multi-layer perceptron neural network and (5) recurrent neural network (RNN) with long short-term memory (LSTM). The models were implemented by using Python's Scikit-Learn [28] and Keras [29] frameworks. The investigated models are briefly described in the following (for a more detailed description see [30] for example).

1) *Linear Least Squares Regression:* The Linear Least Squares algorithm, is based on a linear model. The target output variable is represented as a linear combination of the input variables. The algorithm aims to minimize the squared sum of the difference between the true value in the training dataset and the predicted value by the linear approximation.
2) *k-Nearest Neighbors Regression:* The *k*-Nearest Neighbor (*k*-NN) algorithm uses similarity in the input variables to predict values of new data points. During the training phase, the training data set is only indexed and stored into a database. A new data point is predicted based on how closely it corresponds to the points in the training set. A weighted average of the *k*-nearest neighbors is used to predict the value. The main hyperparameters of the model is *k*, the number of nearest neighbors used for the prediction.
3) *Decision Tree Regression:* Decision Trees models recursively partitioning the input feature space by inferring simple decision rules from the training data set. The data is represented by a tree structure. The branches of the tree are representing the decision rules and the leaves contain the trained values. The main hyperparameters for

Table 1
Prediction performance of the evaluated machine learning models.

Model	History data length	MAE	MAX	RMSE	R^2
Linear Least Square	25	3.19e−03	4.67e−01	1.80e−02	0.94
k-NN	5	5.77e−03	4.73e−01	2.92e−02	0.85
Decision Tree	10	6.61e−03	7.13e−01	3.55e−02	0.76
MLP Neural Network	5	4.56e−03	4.49e−01	2.02e−02	0.89
RNN w/ LSTM	20	3.17e−03	4.65e−01	1.78e−02	0.95

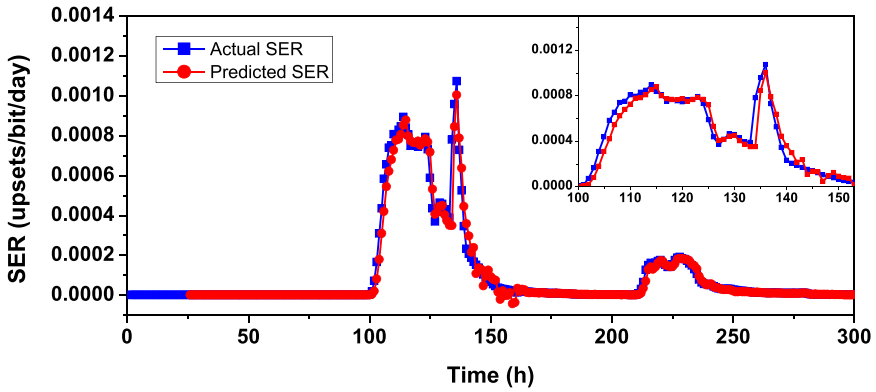

Fig. 6. Prediction of SER over a period of 300 h for one SPE by using linear regression model.

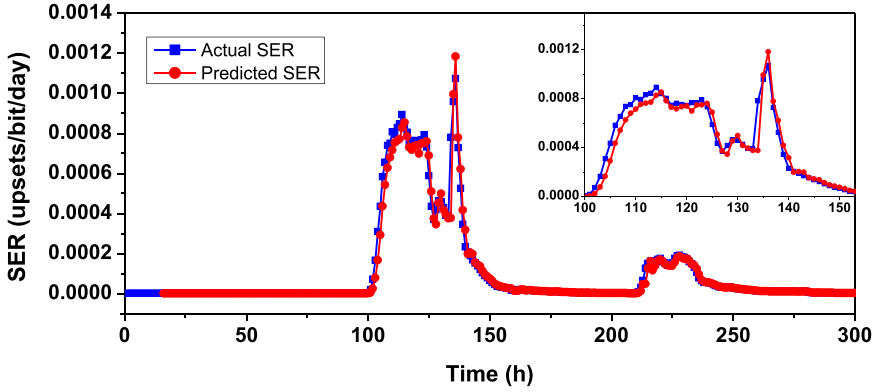

Fig. 7. Prediction of SER over a period of 300 h for one SPE by using RNN with LSTM model.

this model are sued to control the structure of the tree, such as the maximum depth, the maximum number of leaf nodes and the balance of the tree. During the hyperparameter optimisation it has been noted that the model performs at best when the tree structure is not constrained.

4) *Multilayer Perceptron Neural Network:* A multilayer perceptron (MLP) belongs to the class of feedforward artificial neural networks (ANN). An MLP Neural Network consists of at least three layers of nodes. The first layer is the input layer, followed by one or more hidden layers and an output layer. Except for the input nodes, each node is a perceptron. A single perceptron has one or more inputs, a bias, an activation function, and one output. The received input is multiplied by a weight and passed to the activation function, which produces the output. The main hyperparameters for this model are the activation function and the network topology.
5) *Recurrent Neural Network with Long Short-Term Memory:* The Recurrent Neural Network (RNN) is a generalization of feedforward ANN and is extended by an internal memory. This means, that the output of the current input depends on past computations. In the other considered models, all the inputs are independent of each other, but with the help of the RNN's memory, all the inputs are related to each other. The Long Short-Term Memory (LSTM) is a special kind of RNN, to overcome some of its issues to learn dependencies over longer sequences. This means RNN with LSTM are designed to process sequences of input data and this makes them applicable for time series data. The main hyperparameter of this model is, similar to the MLP Neural Network, the network topology.

4.4. Measured model performances

The model performance for each model was measured considering different history length of the hourly SER data. For each considered length the optimal hyperparameter for the model were searched by using the described random and grid search approach and a cross validation fold of 5.

The performance in terms of the R^2 score for each model for a varying history data length is shown in Fig. 5. The maximum R^2 score which can be achieved is 1.0 and lower performance results in lower values. It can be seen that that in general the model performance does not significantly increase with history data length higher than 5. For the k-NN model the performance is even decreasing. The Fig. 5 also shows that the RNN w/ LSTM gives the best performance. Moreover, the linear regression gives almost similar good results.

Table 1 summarizes the best performances for each model (optimal

history data length and optimal hyperparameters). Figs. 6 and 7 show the SER prediction of one SPE from the test data set for the Linear Least Squares and the RNN with LSTM model, respectively. The ´Actual SER´ data in these figures are collected from the solar condition analysis phase, which is the one described in Section 3.

5. Conclusion and future work

In this work, an approach for predicting the in-flight SER variation of the on-board SER monitor system in space applications is proposed. Thus, the upcoming SPEs can be indicated from the rise of predicted SERs at least 1 h in advance. The approach is intended to serve as an enabler of adaptive switching of operating modes within a multi-core processing system. The concept combines the online SER measurement with an SRAM-based particle detector and supervised machine learning prediction model trained offline with publicly available flux databases from past space missions. Preliminary results indicate outstanding of the recurrent neural network (RNN) with long short-term memory (LSTM) machine learning prediction algorithm.

Although the initial results are promising, there are still open issues which have to be addressed in future work in order to make this approach fully operational. The accuracy of the prediction model can be further improved, and the prediction time can be extended beyond 1 h. Then, the optimum hardware implementation of the prediction model should be designed. Moreover, the accuracy can be improved by providing the real-time measurement of the particle energy or LET, which can be used as additional input parameters for the machine learning algorithm. Besides that, it is necessary to integrate the proposed approach in an adaptive multicore system on a single chip, establish a model for estimating the SER of the multicore system in terms of the SER of SEU monitor, and finally test the complete solution under real irradiation.

CRediT authorship contribution statement

J. Chen: Conceptualization, Methodology, Data curation, Software, Validation, Visualization, Writing - original draft. **T. Lange**: Methodology, Data curation, Software, Validation, Visualization, Writing - original draft. **M. Andjelkovic**: Investigation, Formal analysis, Writing - review & editing. **A. Simevski**: Methodology, Writing - review & editing. **M. Krstic**: Resources, Project administration, Supervision.

Declaration of competing interest

The authors declare that they have no known competing financial interests or personal relationships that could have appeared to influence the work reported in this paper.

Acknowledgements

This work has received funding from the European Union's Horizon 2020 research and innovation programme under the Marie Skłodowska-Curie grant agreement No. 722325.

Appendix A. Supplementary data

Supplementary data to this article can be found online at https://doi.org/10.1016/j.microrel.2020.113799.

References

[1] J.L. Barth, et al., Space, atmospheric and terrestrial radiation environments, IEEE Transactions on Nuclear Technology 50 (3) (2003) 466–482.
[2] D.L. Hansen, et al., Correlation of prediction to on-orbit SEU Perfor- mance for a commercial 0.25-μm CMOS SRAM, IEEE Trans. Nucl. Sci. 54 (6) (2007) 2525–2533 Dec.
[3] K.H. Yearby, et al., Single-event upsets in the cluster and double star digital wave processor instruments, Space Weather 12 (1) (2014) 24–28 Jan.
[4] R. Glein, F. Rittner, A. Heuberger, Detection of solar particle events inside FPGAs, 2016 16th European Conference on Radiation and its Effects on Components and Systems (RADECS), Bremen, 2016, pp. 1–5.
[5] A. Simevski, O. Schrape, C. Benito, M. Krstic, M. Andjelkovic, PISA: power-robust microprocessor design for space applications, Proc. IOLTS, 2020.
[6] E. Camporeale, The challenge of machine learning in space weather: nowcasting and forecasting, Space Weather 17 (2019).
[7] H.M. Bain, P. Brea, E.T. Adamson, Using machine learning techniques to forecast solar energetic particles, Proc. SOARS, 2018.
[8] A.J. Engell, D.A. Falconer, M. Schuh, J. Loomis, D. Bissett, SPRINTS: a framework for solar-driven event forecasting and research, Space Weather 15 (10) (2017) 1321–1346.
[9] A. Papaioannou, et al., A novel forecasting system for solar particle Eventa and Flares (FORSPEF), Proc. 24th European Cosmic Ray Symposium (ECRS), 2014.
[10] F. Rocha de Rosa, et al., Using machine learning techniques to evaluate multicore soft error reliability, IEEE Transactions on Circuits and Systems I: Regular Papers, 2019.
[11] T. Lange, A. Balakrishnan, M. Glorieux, D. Alexandrescu, L. Sterpone, Machine learning to tackle the challenges of transient and soft errors in complex circuits, Proc. 25th IEEE International Symposium on Online Testing and Robust System Design, 2019.
[12] S. Hirokawa, et al., Multiple sensitive volume based soft error rate estimation with machine learning, Proc. European Conference on Radiation and its Effects on Components and Systems (RADECS), 2016.
[13] Y. Xu, I. Koren, C.M. Krishna, AdaFT, ACM Trans. Embed. Comput. Syst. 16 (3) (2017) 1–25.
[14] J. Chen, et al., Design of SRAM-based low-cost SEU monitor for self-adaptive multiprocessing system, Proc. 22nd Euromicro Conference on Digital System Design (DSD), Kalithea, Greece, 2019.
[15] P. Hazucha, C. Svensson, Impact of CMOS technology scaling on the atmospheric neutron soft error rate, IEEE Trans. Nucl. Sci. 47 (6) (2000) 2586–2594.
[16] National Oceanic and Atmospheric Administration (NOAA) solar proton events affecting the earth environment lists, [Online]. Available https://ngdc.noaa.gov/stp/satellite/goes/doc/SPE.txt.
[17] Geostationary Operational Environmental Satellites (GOES) - space environment monitor (SEM) database, [Online]. Available https://ngdc.noaa.gov/stp/satellite/goes/dataaccess.html.
[18] Advance composition explorer (ACE) - solar isotope spectrometer (SIS) database, [Online]. Available http://www.srl.caltech.edu/ACE/ASC/level2/lvl2DATA_SIS.html.
[19] S.E. Hoyos, H.D.R. Evans, E. Daly, From satellite ion flux data to SEU rate estimation, IEEE Trans. Nucl. Sci. 51 (5) (2004) 2927–2935 Oct.
[20] A.J. Tylka, et al., CREME96: a revision of the cosmic ray effects on micro-electronics code, IEEE Trans. Nucl. Sci. 44 (6) (1997) 2150–2160 Dec.
[21] CRÈME96 tool, [Online]. Available https://creme.isde.vanderbilt.edu/.
[22] V. Gupta, Analysis of Single Event Radiation Effects and Fault Mechanisms in SRAM, FRAM and NAND Flash: Application to the MTCube Nanosatellite Project, PhD dissertation University of Montpellier, 2017.
[23] E. Petersen, Single Event Effects in Aerospace, Wiley-IEEE Press, 2011.
[24] J.C. Pickel, J.T. Blandford, Cosmic-ray-induced errors in MOS devices, IEEE Trans. Nucl. Sci. 27 (2) (1980) 1006–1015. April.
[25] D.L. Hansen, K. Jobe, J. Whittington, M. Shoga, D.A. Sunderland, Correlation of prediction to on-orbit SEU performance for a commercial 0.25 μm CMOS SRAM, IEEE Trans. Nucl. Sci. 54 (6) (2007) 2525–2533 Dec.
[26] J. Bergstra, Y. Bengio, Random search for hyper-parameter optimization, J. Mach. Learn. Res. 13 (2012) 281–305 Feb.
[27] R. Kohavi, "A study of cross-validation and bootstrap for accuracy estimation and model selection," in Proceedings of the 14th International Joint Conference on Artificial Intelligence - Volume 2, San Francisco, CA, USA, 1995, pp. 1137–1143, Accessed: Jan. 21, 2019 [Online]. Available: http://dl.acm.org/citation.cfm?id=1643031.1643047.
[28] F. Pedregosa, et al., Scikit-learn: machine learning in Python, J. Mach. Learn. Res. 12 (2011) 2825–2830.
[29] F. Chollet, et al., Keras, Online]. Available, 2015. https://keras.io.
[30] K.P. Murphy, Machine Learning: A Probabilistic Perspective, MIT Press, 2012.